Microglia mitigate neuronal activation in a zebrafish model of Dravet syndrome

Alexandre Brenet, Julie Somkhit, Zsolt Csaba, Sorana Ciura, Edor Kabashi, Constantin Yanicostas, Nadia Soussi-Yanicostas

Microglia mitigate neuronal activation in a zebrafish model of Dravet syndrome

Alexandre Brenet[1], Julie Somkhit[1], Zsolt Csaba[1], Sorana Ciura[2], Edor Kabashi[2], Constantin Yanicostas[1#], and Nadia Soussi-Yanicostas[1*#]

[1]NeuroDiderot, Inserm U1141, Université Paris Cité, Hôpital Robert Debré, Paris, France.

[2]University Paris Descartes Hospital Necker-Enfants Malades, Institut Imagine, Paris.

Co-last author

#Corresponding Author:
Dr. Nadia Soussi-Yanicostas
Hôpital Robert Debré, INSERM
48, Bd Sérurier
75019 Paris France,
Tel: +33-1 40 03 19 31
E-mail: nadia.soussi@inserm.fr

Keywords: Microglia, Epilepsy, Seizure, Calcium imaging, Zebrafish, Seizures, Cytokines, Neuroprotection

Running title: microglia remodeling in epilepsy

Abstract

It has been known for a long time that epileptic seizures induce brain neuroinflammation through microglia activation. Nevertheless, these cells have not yet received the attention they deserve in epilepsy research and the consequences of this microglial response on subsequent neuronal activity remain poorly understood. Here, we sought to fill this gap and gain a larger understanding of the role of microglia in the pathophysiology of epilepsy, using an established zebrafish Dravet syndrome epilepsy model based on Scn1Lab sodium channel loss-of-function, combined with live microglia and neuronal Ca^{2+} imaging, local field potential (LFP) recording and genetic microglial ablation. First, in *scn1Lab*-deficient larvae experiencing epileptiform seizures, microglia displayed morphological and biochemical features suggesting M1-like pro-inflammatory activation, including reduced branching, amoeboid-like morphology, and a marked increase in the number of microglia expressing pro-inflammatory cytokine Il1β. More importantly, *scn1Lab*-KD larvae fully lacking microglia showed a significantly increased neuronal activation compared to that seen in *scn1Lab*-KD individuals with microglia, as shown by LFP recording and Ca^{2+} imaging, and also by the epileptiform seizure-related whirling swimming of larvae. These findings are evidence that despite a microglial activation and the synthesis of pro-inflammatory cytokines, microglia provide neuroprotection to epileptic neuronal networks, making these cells a promising therapeutic target in epilepsy.

Introduction

Epilepsy is the most frequent neurological disorder, affecting more than 1% of the world's population (Fisher *et al.*, 2014; Fisher, 2015). The disease is characterized by recurrent seizures caused by synchronized hyperactivation of neuronal networks of various sizes ranging from a limited brain region to the whole cortex, leading to focal or generalized seizures, respectively (Thurman *et al.*, 2011; Stafstrom and Carmant, 2015; World Health Organization, 2019). Potent anti-epileptic drugs (AEDs) have been developed over the last decades. However, they are ineffective in approximately one-third of patients, especially children with developmental epileptic encephalopathies, such as Dravet syndrome (DS) (Brunklaus, Dorris and Zuberi, 2011; Kwan, Schachter and Brodie, 2011; Wu *et al.*, 2015). In addition, they can cause significant side effects, such as teratogenicity in pregnant women (Xue-Ping *et al.*, 2019; Marxer *et al.*, 2021). These limitations emphasize the need for novel anti-epileptic strategies. Notably, most existing AEDs are "neurocentric", targeting neuronal proteins directly involved in neuronal network activation. At the same time, microglia have so far received little attention as a therapeutic target in epilepsy despite large amounts of data accumulated over the last decades, strongly suggesting that these cells are essential players in the pathophysiology of the disease (Vezzani, Balosso and Ravizza, 2019).

Microglial cells, the resident brain macrophages, have several essential functions, including immunoprotection, maintenance of neuron health and homeostasis, and maturation of neuronal networks through developmentally controlled apoptosis of supernumerary neurons and pruning excess synapses (Lukens and Eyo, 2022). As immune cells, microglia also respond rapidly to brain injury or infection through complex reprogramming, referred to as microglia activation, which comprises morphological and biochemical changes, including the synthesis and release of pro-inflammatory cytokines (Woodburn, Bollinger and Wohleb, 2021). In epileptic patients, it has long been known that seizures cause the activation of microglial cells and synthesis of inflammatory mediators (Ravizza *et al.*, 2008; Vezzani *et al.*, 2008; Vezzani, 2013; Vezzani, Balosso and Ravizza, 2019). Analysis of post-mortem brain tissues from epileptic patients has indeed shown massive microglial activation, directly correlated with seizure severity (Boer *et al.*, 2008; Morin-Brureau *et al.*, 2018). Moreover, in various pharmacological rodent epilepsy models, pronounced morphological changes of microglia were rapidly observed after seizures, prior to the onset of neuronal damage (Eyo *et al.*, 2014; Avignone *et al.*, 2015). However, other studies have highlighted the wide variability of inflammatory responses observed in patients and animal epilepsy models (Gasmi *et al.*, 2021). Some data suggest that microglia may be harmful in an epileptic context, probably owing to the release of pro-inflammatory cytokines, known to be pro-epileptogenic factors (Vezzani *et al.*, 1999; Rana and Musto, 2018; Andoh, Ikegaya and Koyama, 2019). Conversely, other

studies suggest that microglia may play a beneficial role in epilepsy by decreasing the activity of neuronal networks (Li, X. Du, *et al.*, 2012; Vinet *et al.*, 2012; Eyo *et al.*, 2014; Badimon *et al.*, 2020). Data also suggest that the response of microglia to epileptic seizures is not uniform throughout the brain, with cells showing a wide range of phenotypes within the same individual (Morin-Brureau et al., 2018). Moreover, the levels of both pro-inflammatory and anti-inflammatory cytokines are increased in microglia after epileptic seizures, supporting the notion that the response of these cells to seizures is not limited to classic M1-type pro-inflammatory activation, thus highlighting the complexity of this microglial response (Benson et *al.*, 2015). Whether microglia activity has an overall detrimental or beneficial role in epilepsy is still a largely open question with far-reaching therapeutic implications (Lukens and Eyo, 2022).

To address this issue and gain a better understanding of the role of microglia in epilepsy, we used a zebrafish model of Dravet syndrome (DS), a severe intractable epileptic syndrome in infants caused in 70–80% of cases by *de novo* mutations in the gene encoding the voltage-gated sodium channel, *SCN1A* (Claes *et al.*, 2001; Dravet, 2011). We used this zebrafish epilepsy model to investigate the morphology and dynamic behavior of microglial cells *in vivo*, using the Tg[mpeg1:mCherryF] line, which enables imaging of microglial cells in living zebrafish embryos and larvae combined with neuronal Ca^{2+} imaging, local field potential (LFP) recording and genetic microglia ablation.

We found that microglia were deeply remodeled in *scn1Lab*-deficient larvae, with morphology shifted toward the amoeboid and less branched phenotype, combined with a markedly increased mobility of their cell bodies and an increased number of Il1β-expressing cells. In addition, in microglia-depleted *scn1Lab*-deficient larvae, neuronal hyperactivation was significantly increased compared with their siblings with microglia, suggesting that activities of these cells lent neuroprotection to epileptic neurons and decreased their activity.

Results

Microglia morphological changes in *scn1Lab*-KD larvae

To increase our understanding of microglia phenotypes in epileptic brains *in vivo,* we first made use of the live imaging techniques available in zebrafish, especially real-time microglia imaging (Hassan-Abdi *et al.*, 2019), combined with two zebrafish *scn1Lab* models of Dravet syndrome epilepsy, *scn1Lab* morphant (Brenet *et al.*, 2019) and *scn1Lab*$^{s552/s552}$ mutant larvae (Scott C Baraban, Dinday and Hortopan, 2013). Both models show recurrent spontaneous epileptiform seizures at 4 days post-fertilization (dpf), as visualized by LFP recording and Ca^{2+} imaging and by the characteristic swirling behavior of the larvae (Scott C. Baraban, Dinday and Hortopan, 2013; Zhang *et al.*, 2015; Brenet *et al.*, 2019). Specifically, we mainly used *scn1Lab* morphants, referred to below as *scn1Lab*-KD individuals, and verified that the results were identical in *scn1Lab*$^{s552/s552}$ mutants, displaying a complete loss of Scn1Lab function (Scott C. Baraban, Dinday and Hortopan, 2013; Brenet *et al.*, 2019). To visualize microglial cells *in vivo*, we chose the transgenic Tg[*mpeg1*:mCherryF] line, which shows intense labeling of these cells (Travnickova *et al.*, 2015). However, as this transgenic line expresses mCherryF in both microglia and macrophages, we verified that all the microglia imaged in this study also expressed the Tg[p2y12:P2Y12-GFP] transgene (Sieger *et al.*, 2012), as P2RY12 is a specific marker of microglial cells (Mildner, 2017).

As previously shown (Peri and Nüsslein-Volhard, 2008; Hassan-Abdi *et al.*, 2019), in wild-type (WT) larvae, microglia displayed the characteristic branched morphology of "resting" microglia, with a relatively small cell body and several long and ramified processes (**Figure 1A; 1A1-3 and Supp. Fig. 1A$_2$ (Video 1): https://urlz.fr/iPxZ**). By contrast, in *scn1Lab*-KD larvae, microglia exhibited a more rounded morphology, with a larger cell body combined with fewer and shorter branches (**Figure 1B; 1B1-3 and Supp. Fig. 1B$_3$ (Video 2): https://urlz.fr/iPxP**). To further characterize the morphological differences in the two genetic contexts, we used the 3D image analysis software Imaris (Bitplane) to measure several microglial cell morphological parameters (sphericity, volume, surface area, branch number, branch length and ramification index). Data confirmed that microglia in *scn1Lab*-KD larvae displayed an increased sphericity (WT: 0.567 ± 0.006 *vs. scn1Lab*-KD: 0.644 ± 0.006; $p < 0.0001$) (**Figure 1C**), a decreased number of branches (WT: 6.3 ± 0.2 *vs. scn1Lab*-KD: 5.1 ± 0.2; $p < 0.0001$) (**Figure 1D**), a decreased total (WT: 115 ± 3 µm *vs. scn1Lab*-KD: 85 ± 3 µm; $p < 0.0001$) (**Figure 1E**) and mean processes length (control: 23.5 ± 0.4 µm *vs. scn1Lab*-KD: 19.6 ± 0.3 µm; $p < 0.0001$) (**Figure 1F**), and a decreased ramification index (WT: 1.94 ± 0.05 *vs. scn1Lab*-KD: 1.74 ± 0.05; $p < 0.0001$) (**Figure 1G**) compared with microglia in WT individuals. Sholl analysis, a method used to quantify both the extent and complexity of cell branches (Imaris software), further confirmed that microglia in *scn1Lab*-KD individuals had fewer and shorter branches

than their WT siblings (**Figure 1H**). Taken together, our data show that microglia exhibited an amoeboid-like morphology reminiscent of that of M1-type activated macrophages in *scn1Lab*-KD larvae.

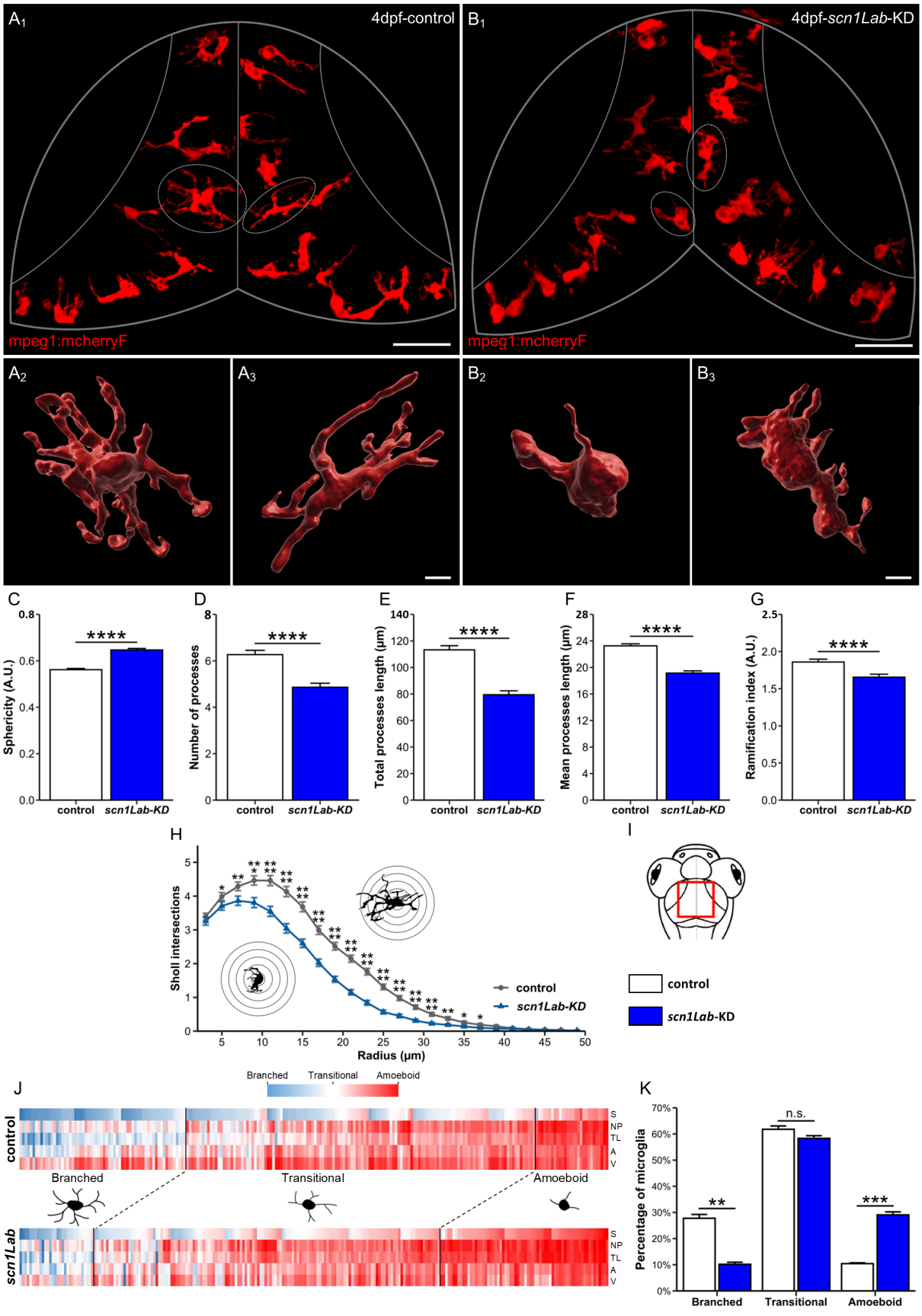

***Figure 1*: Microglial morphology in the *scn1Lab* model.**

(**A-B**) Dorsal view of 4 dpf Tg[mpeg1:mCherryF] control (**A_1**) and *scn1Lab*-KD (**B_2**) larvae optic tectum showing microglial cell population, as well as 3D reconstruction of control (**A_2-A_3**) and *scn1Lab*-KD (**B_2-B_3**) microglia. (**C-G**) Quantification of microglial cells' sphericity (**C**), number of processes (**D**), total processes length (**E**), mean processes length (**F**) and ramification index (**G**) in 4 dpf *scn1Lab*-KD larvae (N = 11; n = 239) compared to sibling controls (N = 11; n = 228). (**H**) Sholl analysis of control (grey) and *scn1Lab*-KD (blue) microglia. (**I**) Diagram of the head of a zebrafish larva with the area of interest (the periventricular stratum) framed in red. (**J**) Cluster analysis of the microglial population of 4 dpf *scn1Lab*-KD (N = 11; n = 239) and sibling control (N = 11; n = 228) based on sphericity (S), number of processes (NP), total processes length (TL), area (A), and volume (V), leading to three microglial populations. (**K**) Repartition of the control (white) and *scn1Lab*-KD (blue) microglial population in the three clusters produced before. All images were acquired with SP8 Leica scanning laser confocal equipped with 20x/multi-immersion 0.75 objective. All data are represented as the mean ± sem. p-values were determined using Mann-Whitney or unpaired Student t-test depending on the normal distribution of the values. n.s., non-significant; **, $p < 0.01$; ***, $p < 0.001$; ****, $p < 0.0001$. Scale bars: 50 µm (A_1, B_1); 10 µm (A_2, A_3, B_2, B_3).

To better evaluate the extent of microglia morphological differences in *scn1Lab*-KD and WT larvae, we performed a cluster analysis of these cells in the two genetic contexts based on the five morphological parameters showing significant changes as indicated above (sphericity, branch number, branch length, surface area, and volume) (see Materials and Methods). The first population comprised cells showing low sphericity, numerous elongated branches, and high surface area and volume, referred to below as "branched" microglia. The second comprised microglia displaying high sphericity, few short processes, and low surface area and volume, referred to below as "amoeboid" cells. The third comprised cells with intermediate characteristics, referred to below as "transitional" microglia (**Figure 1J**). Although the three populations of microglia were found in both contexts, their respective proportion varied considerably. In *scn1Lab*-KD larvae, we observed a significant increase in the percentage of "amoeboid" microglia (29.1 ± 1.2 *vs.* 10.4 ± 0.3%; $p < 0.001$) combined with a significant decrease in the percentage of "branched" microglia (10.2 ± 0.8 *vs.* 27.8 ± 1.5%; $p < 0.01$) (**Figure 1K**). These findings further prove that microglia display an M1-like reactive phenotype in *scn1Lab*-KD larvae.

Visual examination of the behavior of microglia in *scn1Lab*-KD and WT larvae provided a first indication that these cells displayed an increased mobility in the mutant context. To confirm this observation, we measured the speed of microglia cell bodies in the two genetic contexts. In WT larvae, as previously described (Hassan-Abdi *et al.*, 2019), microglia had several branches that were constantly extending and retracting, while their cell bodies remained almost

immobile (**Figure 2A$_1$-A$_2$, 2C$_1$, 2F$_1$**) (**Supp. Video 3,** https://urlz.fr/iOIz). By contrast, cell bodies of *scn1Lab*-KD microglia were much more mobile (**Figure 2B$_1$-B$_2$, 2C$_2$, 2F$_2$**) (**Supp. Video 4,** https://urlz.fr/iOIA).

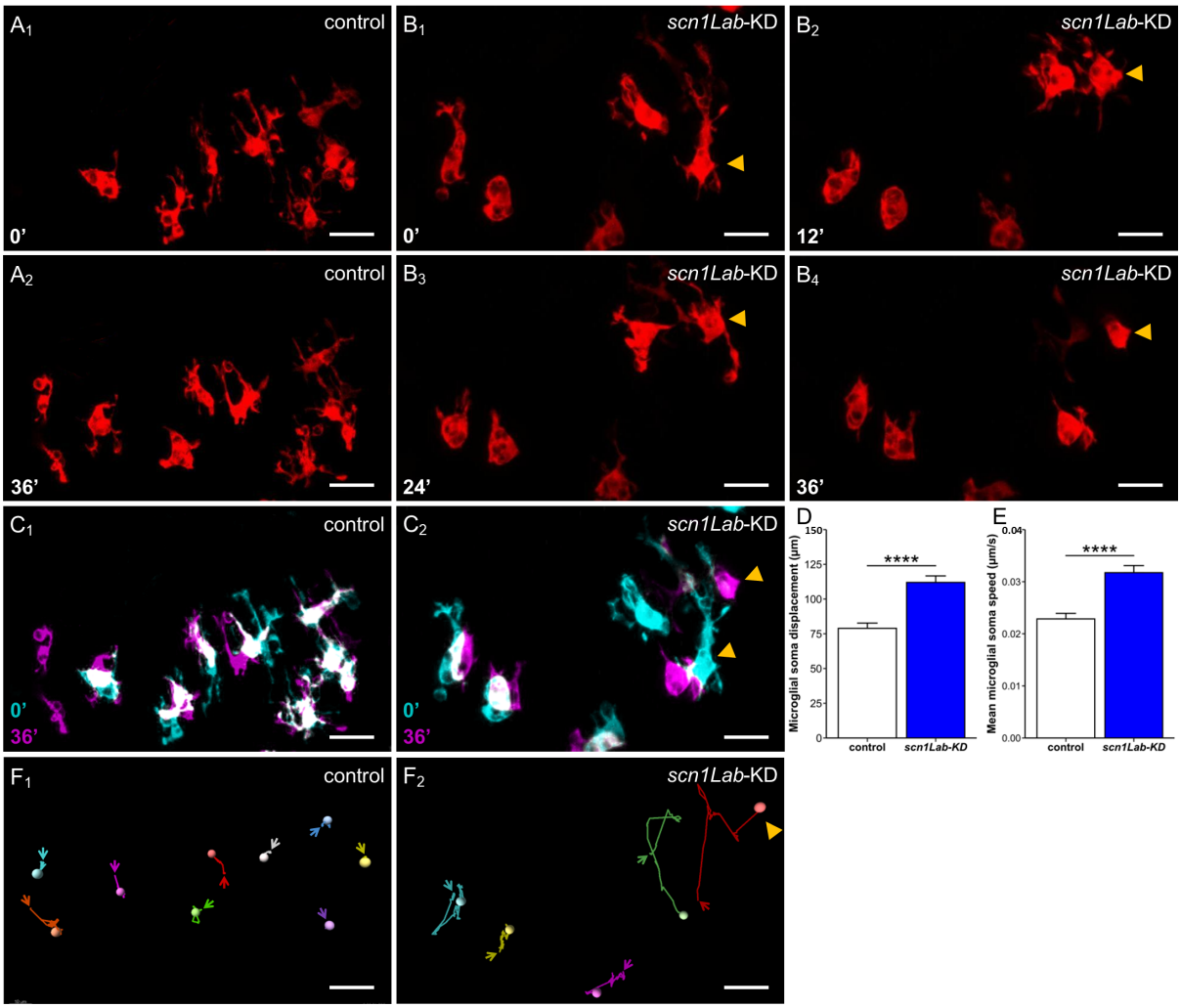

***Figure 2*: Microglial dynamics in the *scn1Lab* model.**

(**A**) Confocal time-lapse showing microglial dynamic in a 4 dpf Tg[mpeg1:mCherryF] control living larval brain. (**B**) Confocal time-lapse showing microglial dynamic in a 4 dpf Tg[mpeg1:mCherryF] *scn1Lab*-KD living larval brain. (**C**) Merged image of two-time points highlighting the increase in microglial soma displacement in *scn1Lab*-KD larvae (**C$_2$**) compared to sibling control (**C$_1$**) (0': cyan, 36': magenta, merge: white). (**D-E**) Quantification of microglial cell body displacement (**D**) and mean displacement speed (**E**) over 60' recording in 4 dpf *scn1Lab*-KD larvae (N = 6; n = 55) compared to sibling controls (N = 4; n = 46). (**F**) Microglial cell tracking over 60' in 4 dpf control (**F$_1$**) and *scn1Lab*-KD (**F$_2$**) living larval brain. Scale bar 20 µm in all images. N = number of larvae and n = number of microglial cells. All images were acquired with a SP8 Leica laser scanning confocal equipped with a 40x/water 1.1 objective. All data are represented as the mean ± sem. p-values were determined using Mann-Whitney test. ****, $p < 0.0001$.

Increased microglia-mediated brain inflammation in *scn1Lab*-KD larvae

Because the microglia phenotypic changes observed in *scn1Lab*-KD larvae were strongly reminiscent of those of “activated” M1-type neuroinflammatory microglia observed in various neuronal disease situations, including epilepsy (Morin-Brureau *et al.*, 2018), we next evaluated the neuroinflammatory profile in the brain of *scn1Lab*-KD larvae. First, we used qRT-PCR to quantify the brain accumulation of transcripts encoding two key pro-inflammatory cytokines, interleukin-1β (Il1β*)* and interleukin-8 (Il8), and three anti-inflammatory cytokines, interleukin-10 (Il10), interleukin-4 (Il4) and transforming growth factor β-3 (Tgfβ3). Surprisingly, we did not observe any significant changes, neither in the expression of pro-inflammatory markers *il1β* (WT: 1.00 ± 0.22 *vs. scn1Lab*-KD: 1.33 ± 0.18; $p > 0.05$) and *il8* (WT: 1.00 ± 0.09 *vs. scn1Lab*-KD: 0.93 ± 0.11; $p > 0.05$) (**Figure 3A**), nor in that of anti-inflammatory markers *il10* (WT: 1.00 ± 0.21 *vs. scn1Lab*-KD: 0.767 ± 0.17; $p > 0.05$), *il4* (WT: 1.00 ± 0.12 *vs. scn1Lab*-KD: 0.89 ± 0.19; $p > 0.05$) and *tgfβ3* (WT: 1.00 ± 0.04 *vs. scn1Lab*-KD: 0.876 ± 0.08; $p > 0.05$) (**Figure 3B**). Therefore, although morphological changes seen in *scn1Lab*-KD larvae suggested pro-inflammatory microglial activation, no significant increase in the expression of pro- or anti-inflammatory cytokines could be detected in the brain of these individuals. It may be that in this genetic model of epilepsy, levels of neuroinflammation are lower than those observed in rodent pharmacological models, as also suggested by the relatively small percentage of amoeboid microglia in *scn1Lab*-KD individuals (~30%). To analyze more precisely the microglial expression of Il1β in this genetic context, we generated *scn1Lab*-KD larvae also expressing the Tg[*mpeg1*:mCherryF] and Tg[*il1β*:GFP] transgenes (Nguyen-Chi *et al.*, 2015). The results revealed a significant increase in the percentage of microglia expressing Il1β (WT: 14.6 ± 1.7 *vs. scn1Lab*-KD: 33.6 ± 1.7%; $p < 0.0001$) (**Figure 3C-F**). These results confirmed an increased number of activated microglial cells in *scn1Lab*-KD larvae, consistent with the increased number of "amoeboid" microglia previously characterized.

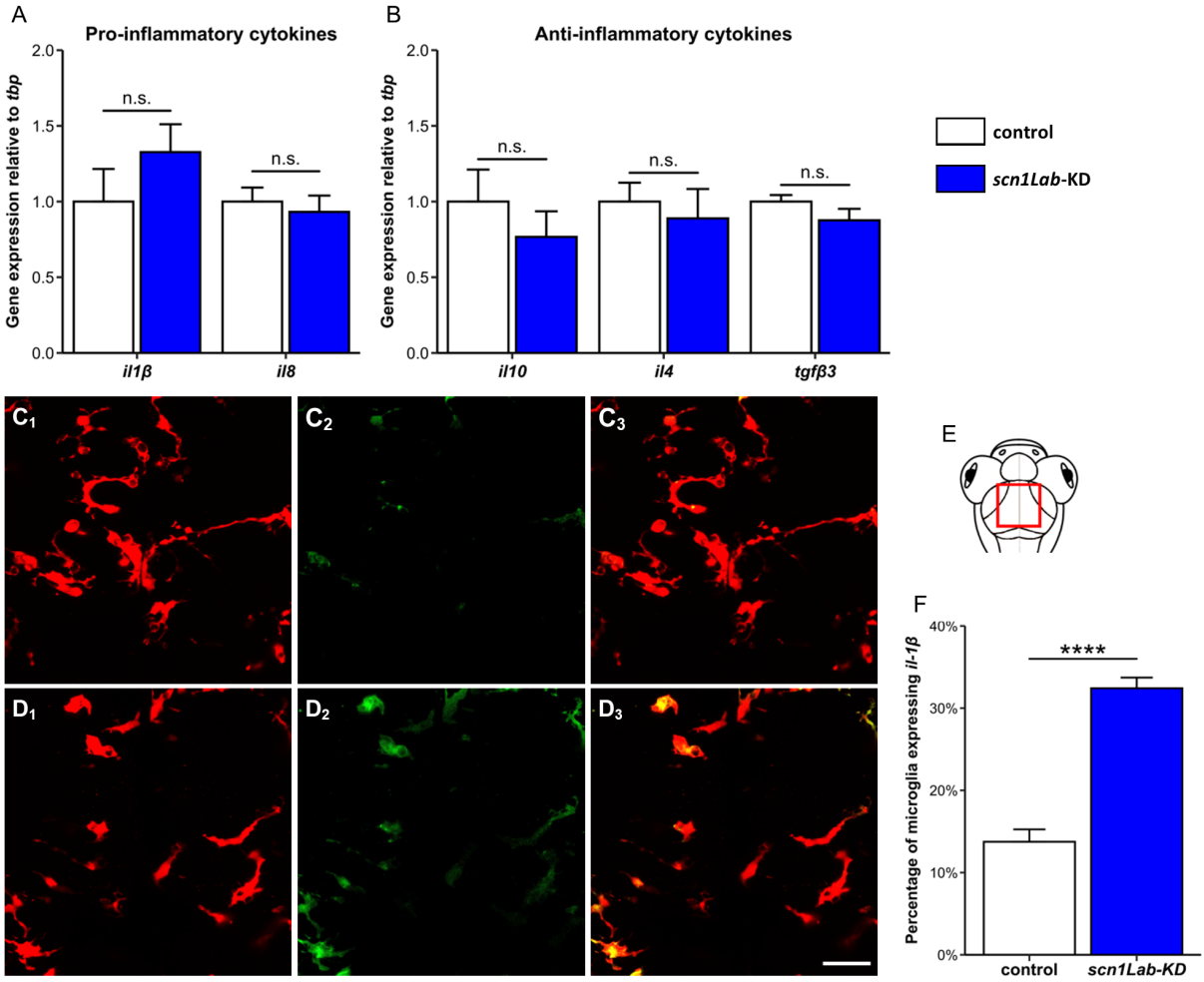

***Figure 3*: Study of the inflammatory profile of *scn1Lab*-KD larvae.**

(**A**) Quantification of the expression of genes encoding pro-inflammatory cytokines, Il1β and Il8, relative to that of the *tbp* gene, in the brain of control (white) and *scn1Lab*-KD (blue) larvae, aged 4 dpf. (**B**) Quantification of the expression of the genes encoding the anti-inflammatory cytokines, Il10, Il4, and Tgfβ3, relative to that of the *tbp* gene, in the brain of control (white) and *scn1Lab*-KD (blue) larvae aged 4 dpf. (**C**-**D**) Dorsal view of the periventricular stratum of control (**C**) and *scn1Lab*-KD (**D**) 4 dpf larvae, showing microglial cells (**C_1**, **D_1**), Il1β protein expression (**C_2**, **D2**), as well as the superposition of the two signals (**C_3**, **D_3**). (**E**) Diagram of the head of a zebrafish larva with the area of interest (the periventricular stratum) framed in red. (**F**) Quantification of the percentage of microglial cells expressing the cytokine Il1β in control larvae (*N* = 19) and *scn1Lab*-KD (*N* = 16). Scale: 10 µm. *N* = number of larvae analyzed. All images were acquired using a Leica SP8 confocal microscope, equipped with a 20x/water objective with a numerical aperture of 0.75. All graphs represent mean ± sem. The *p*-values were calculated using a Student's *t*-test. n.s., not significant; ****, p<0.0001.

Microglia ablation increases neuronal activation in *scn1Lab*-KD larvae

The phenotypic changes and Il1β expression observed in microglia of *scn1Lab*-KD larvae strongly suggest that a small, albeit significant, proportion of microglia, approximately 30% of

the cells, respond to neuronal seizures through M1-type pro-inflammatory activation. These results then raised the question of whether this microglial response globally mitigates or worsens subsequent activity of neuronal networks. As a first attempt to address this question, we generated *scn1Lab*-KD larvae expressing the Tg[*HuC*:GCaMP5G] transgene, a sensitive calcium bio-sensor (Akerboom *et al.*, 2012), and entirely devoid of microglia following morpholino-mediated inactivation of the *pU.1* gene, which encodes a factor essential for proper differentiation of macrophages and microglia (Rhodes *et al.*, 2005; Peri and Nüsslein-Volhard, 2008). As previously described (Peri and Nüsslein-Volhard, 2008), the brain of larvae injected with *PU.1* morpholinos are devoid of microglia, as shown by the absence of L-plastin immunostaining (**Figure 4A$_2$**) compared with non-injected larvae (**Figure 4A$_1$**). With these tools, we analyzed and compared neuronal activation in WT and *scn1Lab*-KD larvae, devoid or not of microglia, using calcium imaging and local field potential (LFP) recordings simultaneously.

As previously shown (Brenet *et al.*, 2019; Liu and Baraban, 2019), when compared to WT individuals, *scn1Lab*-KD larvae display a markedly increased neuronal activity as indicated by the larger number of seizure-like events revealed by either calcium imaging (WT: 16.5 ± 1.0 *vs. scn1Lab*-KD: 32.2 ± 1.4, $p < 0.0001$) (**Figures 4B, 4D$_1$**) and (**Supp. Video 5,** https://urlz.fr/jlSX**), (Supp. Video 6,** https://urlz.fr/jlT1) and LFP recording (WT: 4.8 ± 1.2 *vs. scn1Lab*-KD: 28.2 ± 2.4, $p < 0.0001$) (**Figures 4C, 4E$_1$**). More importantly, microglia depletion increased the amplitude of neuronal events in both WT and *scn1Lab*-KD larvae (**Figure 4D$_2$, 4E$_2$**) and (**Supp. Video 7,** https://urlz.fr/jlTa), **(Supp. Video 8,** https://urlz.fr/jlTr), and exacerbated the number of epileptiform events in *scn1Lab*-KD individuals, suggesting that microglia displayed a neuroprotective activity that was able to mitigate, at least partially, neuronal hyperactivation.

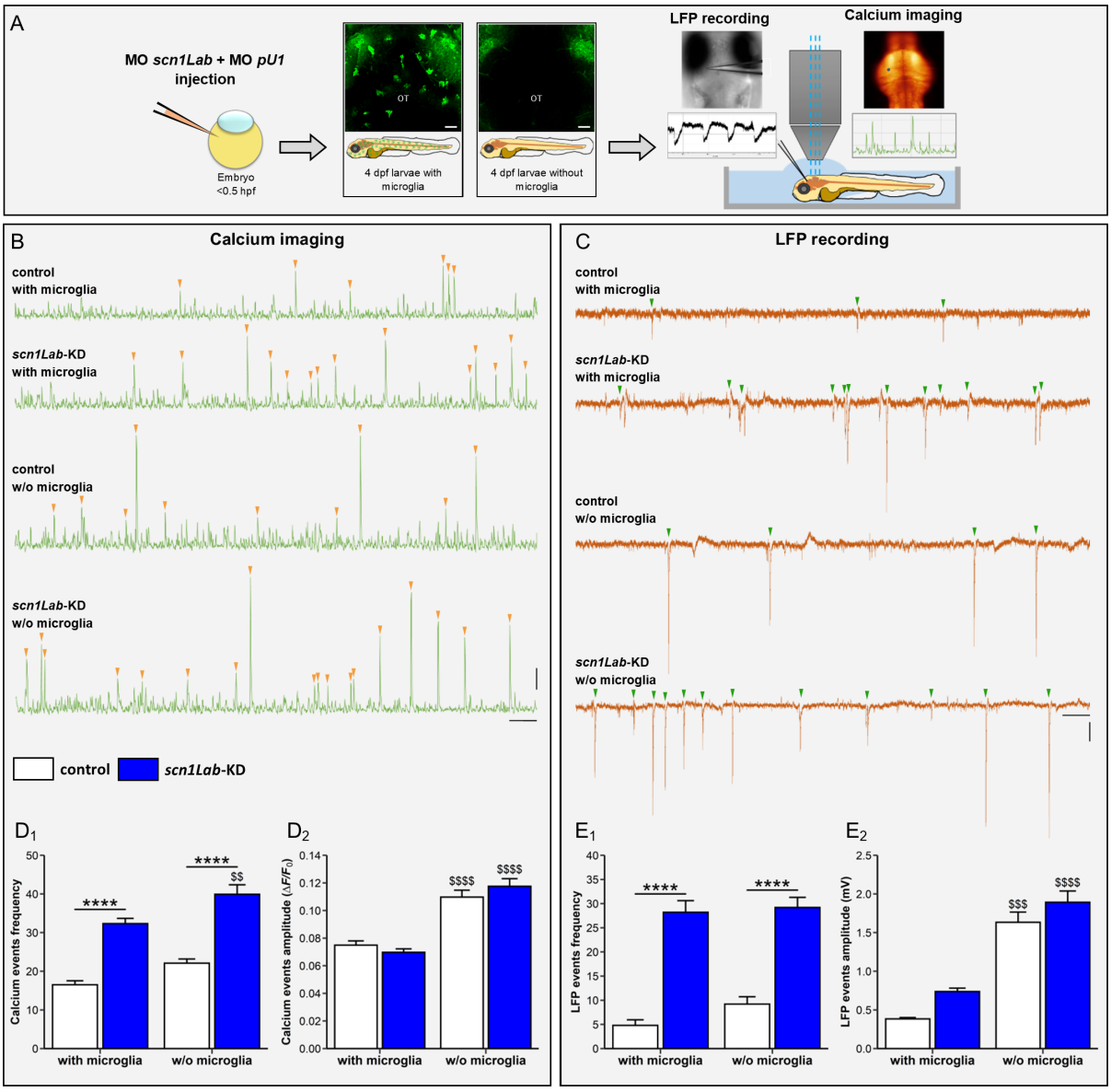

***Figure 4*: Consequences of microglial genetic depletion on neuronal activity in the *scn1Lab* model.**

(**A**) Schematic of the experimental setup. (**B**) 20 min representative calcium traces of 4 dpf control (*N* = 11), *scn1Lab*-KD (*N* = 16), control without microglia (*N* = 9) and *scn1Lab*-KD without microglia (*N* = 9) larvae (from top to bottom). (**C**) 20 min representative LFP traces of 4 dpf control (*N* = 5), *scn1Lab*-KD (*N* = 5), control without microglia (*N* = 5) and *scn1Lab*-KD without microglia (*N* = 5) larvae (from top to bottom). Scale bars of calcium traces: 0.05 $\Delta F/F_0$ and 1 min; of LFP traces: 0.5 mV and 1 min. (**D**) Quantification of calcium events, fluorescence increase greater than 0.04 $\Delta F/F_0$, frequency (**D**$_1$), and amplitude (**D**$_2$) during 1-hour recording in 4 dpf control (white) and *scn1Lab*-KD (blue) larvae. (**E**) Quantification of LFP events, downwards depolarization greater than 0.3 mV and lasting more than 100 ms, frequency (**E**$_1$), and amplitude (**E**$_2$) during 1-hour recording in 4 dpf control (white) and *scn1Lab*-KD (blue) larvae. *N* = number of larvae. All data are represented as the mean ± sem. ****, $p < 0.0001$:

indicates a statistically significant difference between control and *scn1Lab*-KD larvae. $$, $p < 0.01$; $$$, $p < 0.001$; $$$$, $p < 0.0001$: indicates a statistically significant difference between larvae with or without microglial cells. *p*-values were determined using two-way ANOVA with Tukey post-tests.

Microglia ablation exacerbates seizure-like swimming behavior of *scn1Lab*-KD larvae

It has been shown that *scn1Lab* mutant and morphant exhibit spontaneous seizure-like swimming behavior consisting of whole-body convulsions and rapid undirected movements (Scott C. Baraban, Dinday and Hortopan, 2013; Brenet *et al.*, 2019). Therefore, we questioned whether the locomotor activity of *scn1Lab*-KD larvae was dependent on microglia (**Figure 5A**). As previously shown, *scn1Lab*-KD larvae swam longer and over longer distances than WT (WT: 212 ± 11 *vs.* *scn1Lab*-KD: 355 ± 11 mm, $p < 0.0001$), reflecting their neuronal hyperactivation (**Figures 5F, 5G, 5H**). Interestingly, in *scn1Lab*-KD larvae devoid of microglia, we observed a markedly increased locomotor activity compared with that observed in *scn1Lab*-KD individuals not microglia-depleted (*scn1Lab*-KD: 355 ± 11 *vs.* microglia-depleted *scn1Lab*-KD: 423 ± 12 mm, $p < 0.0001$) (**Figures 5B-D**), suggesting that microglia depletion worsened the locomotor behavior of *scn1Lab*-KD larvae thus confirming that neuronal activation was exacerbated in *scn1Lab*-KD larvae lacking microglia compared to that observed in *scn1Lab*-KD individuals.

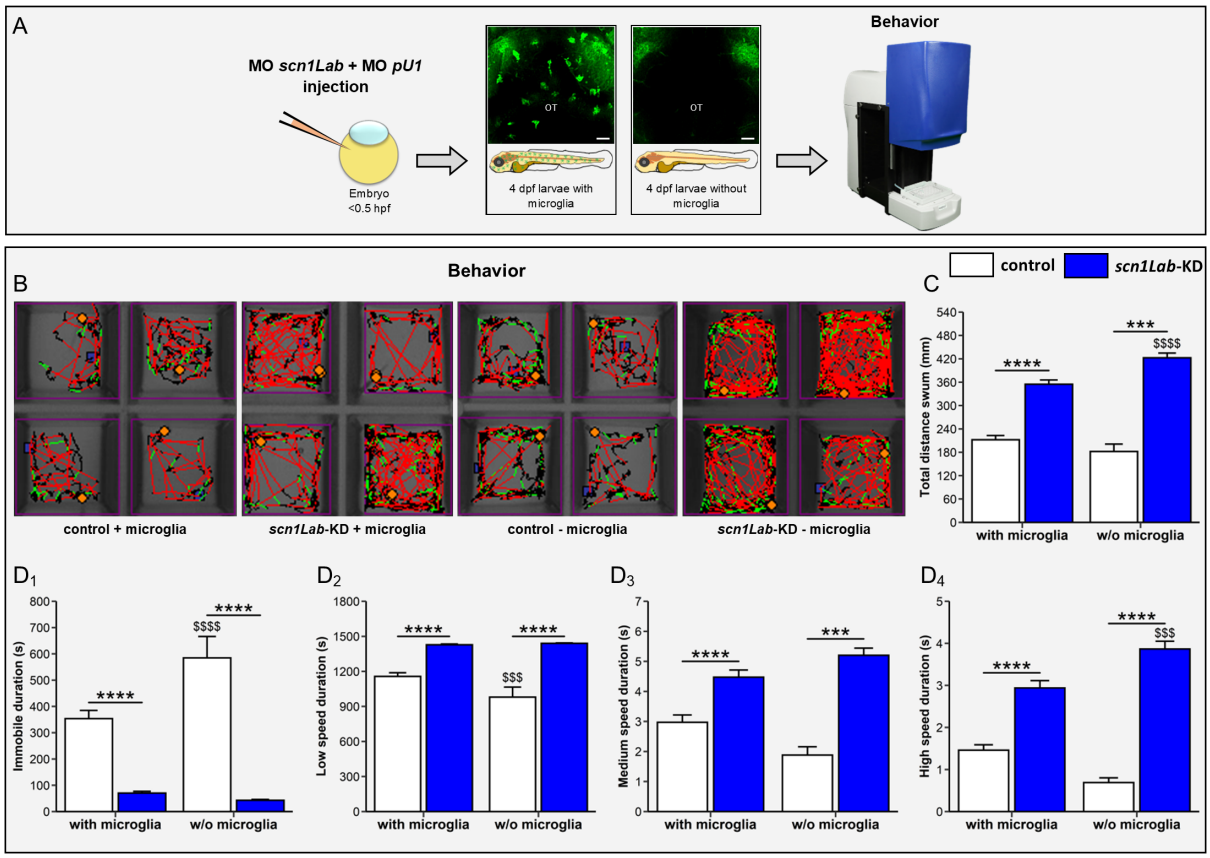

***Figure 5*: Consequences of genetic ablation of microglia on the locomotor activity of *scn1Lab*-KD larvae.**

(**A**) Diagram describing the experimental protocol. (**B**) Plots of distances traveled by control larvae (N = 148), *scn1Lab*-KD (*N* = 184), controls without microglia (*N* = 45) and *scn1Lab*-KD without microglia (*N* = 288) (from right to left). The swimming speed is represented according to the following color code: black represents a low speed, green a medium speed, and red a high speed. (**C**) Quantification of the total distance traveled by 4 dpf control (white) and *scn1Lab*-KD (blue) larvae during the 30 minutes recording. (**D**) Quantification of the time spent by 4 dpf control (white) and *scn1Lab*-KD (blue) larvae in a motionless position ($\mathbf{D_1}$), at low ($\mathbf{D_2}$), medium ($\mathbf{D_3}$), and high swimming speed ($\mathbf{D_4}$). *N* = number of larvae. All graphs represent the average ± sem. The *p*-values were calculated by a two-way ANOVA followed by a Tukey post-test. ***, $p < 0,001$; ****, $p < 0,0001$: indicates a statistical difference between genotypes. $$$, $p < 0,001$; $$$$, $p < 0,0001$: indicate significant differences depending on the presence or absence of microglia.

Discussion

A close relationship between epileptic seizures and microglia-mediated brain inflammation was established long ago (Vezzani *et al.*, 2004). However, the precise response of microglia to epileptic seizures and its consequences on subsequent neuronal network function have been scantly studied so far, especially in *in vivo* models. Furthermore, it has not been known whether seizure-induced microglia activities reduce or exacerbate neuronal network activity (Lukens and Eyo, 2022). This knowledge gap has several causes, one being that microglia cannot be imaged *in vivo* through the skull in rodents and most other animal species. Transparent windows must be cut, involving delicate surgery and risks of brain trauma that can influence the state of microglia, which are highly sensitive to disturbances in brain homeostasis (He *et al.*, 2018). Zebrafish larvae offer a helpful alternative model because they are transparent, enabling easy imaging of microglial cells in real-time, in a living brain and in its physiological environment (Peri and Nüsslein-Volhard, 2008).

Another difficulty has been that most studies investigating microglia activities in rodent epilepsy models have been conducted using pharmacologically-induced seizures. Those chemicals can then cause extended *status epilepticus*-like activity, usually lasting several hours (Ravizza *et al.*, 2008; Avignone *et al.*, 2015; Vezzani, Balosso and Ravizza, 2019; Maupu *et al.*, 2021), and evoke much stronger brain inflammation than that observed in genetic models, and probably human patients (Gasmi *et al.*, 2021; Maupu *et al.*, 2021; Somkhit, Yanicostas and Soussi-Yanicostas, 2022). This difficulty can be overcome by using a genetic epilepsy model. We report here what is, to our knowledge, the first study of the response of microglial cells *in vivo* in such a model.

We chose an established zebrafish model of Dravet syndrome (DS), a severe epileptic encephalopathy caused by a deficit in the activity of inhibitory interneurons, most commonly caused by *de novo* loss-of-function mutations in the *SCN1A* gene encoding the voltage-gated sodium channel NaV1.1. This zebrafish DS model is based on the loss-of-function of one of the two zebrafish orthologues of the *SCN1A* gene, *scn1Lab*. Mutants and morphants *scn1Lab* larvae display recurrent epileptiform seizures from 3 dpf onward, which we and others had previously characterized (Scott C. Baraban, Dinday and Hortopan, 2013; Brenet *et al.*, 2019). In particular, we previously showed that loss of *scn1Lab* function induced a shift in the excitatory/inhibitory balance, with a decreased number of GABAergic synapses and an increased number of glutamatergic ones, combined with an increased number of apoptotic neurons (Brenet *et al.*, 2019).

In close agreement with findings in both preclinical animal models and human patients (Altmann *et al.*, 2022), microglia displayed significant morphological differences in *scn1Lab*-KD larvae compared to their wild-type siblings. In the mutant context, we observed a decreased

number of “branched” microglia and an increased percentage of microglia showing an amoeboid morphology. These “amoeboid” microglia probably correspond to the previously described M1-type pro-inflammatory “activated” cells observed after brain injuries or in various neuronal disease situations including epilepsy (Morin-Brureau *et al.*, 2018), but also following intoxication by neurotoxic compounds, such as organophosphates (Nakajima and Kohsaka, 2001; Somkhit, Yanicostas and Soussi-Yanicostas, 2022). Interestingly, although the disease was associated with an increased number of microglia with an “activated” phenotype, the proportion of “transitional” microglia was similar in the two genetic contexts, and a small percentage of “resting” microglia was still observed in *scn1Lab*-KD individuals. These observations highlight the complexity of the microglial response in epilepsy and, more importantly, are evidence that different populations of microglial cells are present in epileptic brains, each likely playing a distinct role in the pathophysiology of the disease. Although increased expression of pro-inflammatory mediators has been observed both in patients with different forms of epilepsy and in various animal models (Leal *et al.*, 2017; Morin-Brureau *et al.*, 2018), other studies have shown that anti-inflammatory cytokines are also increased in the epileptic brain (Benson, Manzanero and Borges, 2015). All evidence of a complex response of microglia to epileptic seizures.

Surprisingly, and in contrast with reports in most rodent epilepsy models, qRT-PCR analysis found no significant overexpression of pro-inflammatory cytokine-encoding genes, *il1β* and *il8*, in the brain of *scn1Lab*-KD individuals. This result is probably due to the moderate severity of the seizures in these larvae compared with those induced by pharmacological agents, such as PTZ, kainate, or DFP (Maupu *et al.*, 2021; Somkhit, Yanicostas and Soussi-Yanicostas, 2022), whatever the model species. However, using the transgenic Tg[il1β:GFP] line, which enables Il1β-expressing cells to be visualized (Nguyen-Chi *et al.*, 2015), we observed a significant increase in the percentage of microglia expressing Il1β in *scn1Lab*-KD individuals compared with their WT siblings. This observation, which is in close agreement with our cluster analysis, further confirmed not only the increased number of M1-like “activated” microglia in *scn1Lab*-KD larvae, but also the existence of at least two distinct microglia populations, with and without expression of Il1β. However, the increased expression of il1β was probably too weak to be detected by qRT-PCR analysis of brain RNAs, highlighting the differences between genetic and pharmacological epilepsy models again (Maupu *et al.*, 2021; Somkhit, Yanicostas and Soussi-Yanicostas, 2022). It is also of note that studies of microglia-mediated neuroinflammation in *Scn1A*$^{+/-}$ mice yielded widely varying results. In some studies, significant activation of microglial cells was observed in the prefrontal cortex and dentate gyrus, combined with an increased expression of the *Il1β* and *Tnfα* genes (Satta *et al.*, 2021), while in other studies, no microglia activation was detected in the hippocampus of *Scn1A*$^{+/-}$ mice associated with a lack of over-expression of pro-inflammatory mediators (Salgueiro-Pereira *et*

al., 2019). Furthermore, Benson et al. (2015) showed that whereas microglia expressed both pro- and anti-inflammatory mediators in the mouse pilocarpine model, only pro-inflammatory mediators were overexpressed in microglia of mice exposed to kainate (Benson, Manzanero and Borges, 2015). Complex alterations in microglial M1/M2 markers during the development of epilepsy in two mouse models highlight the wide variety of microglial responses to seizures.

Genetic depletion of microglia in *scn1Lab*-KD larvae exacerbated the hyper-activity of neuronal networks, as shown by the increased number of spontaneous epileptiform seizures and worsening of the characteristic swirling swimming behavior. These results thus suggest that microglia played a protective role in epileptic brains and mitigated neuronal activity. Like ours, other studies have concluded that microglia play a beneficial role in epilepsy through mitigation of neuronal activity and modulation of synaptic plasticity (Mirrione *et al.*, 2010; Li, X. F. Du, *et al.*, 2012; Badimon *et al.*, 2020). In addition, Mirrione et al. (2010) showed that total microglia ablation in adult mice led to an increased sensitivity to the pro-convulsant substance pilocarpine (Mirrione *et al.*, 2010), further evidence that microglia display neuroprotective functions in an epileptic context. However, preventing microglia proliferation using the selective CSF1-R inhibitor GW2580 during the late stage of the epileptogenesis (but not the early stage) decreased spontaneous seizures in the kainate mouse model (Di Nunzio *et al.*, 2021).

This work extends our understanding of the role of microglia in epilepsy. The principal added value of our study is that it is the first investigation of the response of microglial cells *in vivo* in a genetic epilepsy model. We show that epileptiform seizures rapidly induce microglia reprogramming characterized by significant changes in cell shape and dynamic behavior, and increased expression of pro-inflammatory cytokine Il-1β. However, this reprogramming is partial and concerns only part of the microglia, suggesting that the response of these cells to seizures is complex and not limited to M1-type activation. Importantly, we also show that *scn1Lab*-KD larvae entirely devoid of microglia presented an increased number of seizures, with greater intensity, suggesting that microglia activity lends neuroprotection to epileptic neurons. Future research will be needed to investigate how microglial cells modulate neuronal activity. Indeed, modulating microglial cells activity may offer a novel therapeutic strategy of great potential interest by reducing neuronal hyperactivity in epilepsies.

Materials and Methods

Transgenic lines and fish maintenance

Zebrafish were maintained at 26.5°C in 14 h light and 10 h dark cycles. Embryos were collected by natural spawning and raised at 28.5°C in E3 medium. Developmental stages were determined as hours post-fertilization (hpf) or days post-fertilization (dpf) as previously described. 0.003% 1-phenyl-2-thiourea (PTU) was added at 1 dpf to avoid pigmentation. The *scn1Lab*^{s552} line has been previously described (Schoonheim *et al.*, 2010) and was generously provided by the laboratory of Dr. Herwig Baier. Calcium imaging was performed using Tg[*Huc*: GCaMP5G] (Akerboom *et al.*, 2012). Microglia were visualized using Tg[*mpeg1*: mCherryF] (Ellett *et al.*, 2011) and cytokine Il1β expression using Tg[*il1β*: GFP] (Nguyen-Chi *et al.*, 2015).

All the animal experiments described were conducted at the French National Institute of Health and Medical Research (INSERM), UMR 1141, Paris, in compliance with European Union guidelines for the handling of laboratory animals (http://ec.europa.eu/environment/chemicals/lab_animals/home_en.htm). They were approved by the Direction Départementale de la Protection des Populations de Paris and the French Animal Ethics Committee under reference No. 2012-15/676-0069.

Morpholino knockdown

The following morpholinos, obtained from Gene Tools (Philomath, Oregon, USA), were used in this study: 5'-CTGAGCAGCCATATTGACATCCTGC-3' was used at 0.62 mM to block the *scn1Lab* zebrafish mRNA transcription; 5'-GATATACTGATACTCCATTGGTGGT-3' was used at 0.88 mM to block the *PU.1* zebrafish mRNA transcription. These morpholinos were injected with 0.03 mM rhodamine B dextran and 0.1 mM KCl into embryos at stage 1–2 cells.

Microglia morphology

4 dpf Tg[mpeg1:mCherryF] larvae were paralyzed using 300 µM pancuronium bromide (Sigma Aldrich, Saint-Louis, Missouri, USA) and agar-immobilized in the center of a 35 mm glass-bottom dish. A 100 µm stack of the larval living optic tectum was acquired at 1024 × 1024-pixel resolution using a Leica SP8 laser scanning confocal microscope equipped with a 20×/0.75 multi-immersion objective. Images were processed using AutoQuant X3 (Media cybernetic, Rockville, Maryland, USA) and Fiji ImageJ (NIH) software. Microglial cells' surface area, volume and sphericity were quantified using Imaris MeasurementPro (Oxford Instruments, Abingdon, UK). The number and length of microglial processes and their Sholl analysis were determined using Imaris Filament Tracer (Oxford Instruments, Abingdon, UK).

Clustering of microglial cells

Cluster analysis was performed using sphericity (S), number of processes (NP), total processes length (TL), surface area (A), and volume (V) of microglial cells. Microglial cells with at least three of the following features: sphericity less than 0.5, number of processes greater than 7, total processes length greater than 140 µm, and a surface area greater than 2400 µm² were classified as “branched” microglia. Conversely, microglial cells with at least three of the following features: sphericity greater than 0.7, number of processes less than 3, total processes length less than 60 µm, and surface area less than 1500 µm² were classified as “amoeboid” microglia. Microglial cells with fewer than three “branched” or “amoeboid” characteristics were classified as “transitional” microglia.

RNA isolation and quantitative RT-PCR

For RNA isolation, whole larvae or dissected brains were homogenized using a syringe equipped with a 26G needle (10 brains per sample) using the RNA XS Plus kit (Macherey Nagel, Düren, Germany). Following RNA quantification with a Nanodrop 2000 (ThermoScientific, Waltham, Massachusetts, USA) and RNA integrity assessment using denaturing gel electrophoresis, total RNAs (1 µg) were reverse transcribed into cDNAs using the iScript cDNA Synthesis Kit (Bio-Rad, Germany) and qPCRs were performed using iQ SYBR Green Supermix (Bio-Rad, Germany). Samples were run in triplicate and expression levels of the studied genes were normalized to that of the *tbp* gene. The primers (Eurofins Genomics, Ebersberg, Germany) used are listed in Supplementary Table 1.

Microglial dynamics

4 dpf pancuronium bromide-paralyzed Tg[mpeg1:mCherryF] larvae were agar-immobilized in the center of a 35 mm glass-bottom dish. A 42 µm stack of the larval living half optic tectum was acquired at 1024 × 512-pixel resolution every 40 s for 1 h using a Leica SP8 laser scanning confocal microscope equipped with 40×/1.1 water objective (Leica, Wetzlar, Germany). Videos were processed using ImageJ software. Microglial cell body displacement, distance traveled between the first and the last frame, and microglial cell body speed displacement were quantified using Imaris MeasurementPro.

Calcium imaging

For quantification, 4 dpf Tg[Huc:GCaMP5G] larvae were paralyzed using pancuronium bromide, agar-immobilized in the center of a recording chamber, and placed under a Leica SP8 laser scanning confocal microscope equipped with a 20×/0.75 multi-immersion objective. A single focal plane of the optic tectum was captured at a high frequency for 40 minutes. The mean grey value of each frame was measured using ImageJ software, and fluorescence variation ($\Delta F/F_0$) was calculated using Excel (Microsoft, Redmond, Washington, USA) by

subtracting the mean fluorescence intensity of all frames from the fluorescence intensity of a frame of interest, then normalizing this difference by the mean fluorescence intensity of all frames. The fluorescence drift during recording was corrected by subtracting the background intensity of the surrounding frame. Calcium events were defined as any fluorescence increase greater than 0.04 $\Delta F/F_0$.

For movie illustration (Supp. Video 5, 6, 7, 8), larvae were paralyzed and immobilized as described above. Calcium transient in a single focal plane of the optic tectum of larvae were captured for 5 min, at 5 Hz, using a Yokogawa CSU-X1 spinning disk confocal microscope (Yokogawa, Tokyo, Japan) equipped with a LD LCI Plan-Apochromat 25x/0.8 DIC Imm Korr (UV) objective (Zeiss, Oberkochen, Germany).

Local field potential recording

Local field potential recording was performed as described in Brenet et al., 2019.

Briefly, 4 dpf larvae were paralyzed using pancuronium bromide and agar-immobilized in the center of a recording chamber. A glass electrode filled with artificial cerebrospinal fluid was placed in the right neuropil of the optic tectum. Neuronal activity was recorded for 1 h in current clamp mode at 10 µs sampling interval, amplified with a digital gain of 10, and filtered through a 0.1 Hz high-pass filter and 1 kHz low-pass filter. Recordings were analyzed using Clampfit software (Molecular Devices, San Jose, California, USA). Every downward membrane potential variation under -0.3 mV amplitude and lasting more than 100 ms was defined as an event.

Locomotor activity

Larval locomotor activity was assessed using an infrared automated tracking device (Zebrabox), controlled by ZebraLab software (ViewPoint, Lyon, France). First, 4 dpf larvae were individually spread in a 96-well plate in 200 µL E3 medium. The plate was then placed inside the Zebrabox recording chamber in the dark for 30 minutes of habituation after which larvae were tracked for 30 min divided into one-minute integration time. The animal color was set to dark and detection sensitivity to 12 for tracking. Besides the total distance swum by the larvae, we also recorded the number of times that the larvae were immobile, in low-speed, medium-speed, and high-speed movements, together with the duration of the events. The inactive speed threshold was set at 4 mm and the high-speed threshold at 8 mm. Each experiment replicates comprised at least 16 larvae per condition and was completed at least three times.

Data analysis

Data were analyzed and plotted using R-studio 1.2.5. (Posit, Boston, Massachusetts, USA). Data are presented as mean ± sem. Statistical analysis of Figures 1 and 2 was performed

using the Mann-Whitney test, if data did not follow a normal distribution, or Student's unpaired *t*-test with or without Welch's correction depending on the variance difference. Two-way ANOVA with Tukey post-test was used to analyze data in Figures 3, 4, and 5.

Conflict of Interest

The authors declare that the research was conducted in the absence of any commercial or financial relationships that could be construed as a potential conflict of interest.

Author Contributions: AB performed experiments and contributed to the analyses and interpretation of the data. JS performed qRT-PCR. ZC helped with imaging experiments. SC & EK helped with LFP experiments. CY co-led the project and contributed to the writing of the article. NSY led the project, designed the experimental research, and contributed to interpreting the data and writing the manuscript. All authors have read and agreed to the published version of the manuscript.

Funding: This work was supported by the Institut National de la Santé et de la Recherche Médicale (INSERM), and the National Centre for Scientific Research (CNRS). Funding sources had no involvement in the study design, collection, analysis, or interpretation of data, nor in the decision to publish.

Acknowledgments: We thank Francesca Peri (University of Zurich, Switzerland) for providing us with the Tg(p2y12:P2Y12-GFP) transgenic line and George Lutfalla (University of Montpellier, France) for providing us with the Tg(il1β:GFP). We also thank Christiane Romain and Olivier Bar (INSERM UMR 1141) for their technical assistance.

Conflicts of Interest: The authors declare no conflict of interest.

Supplementary figures

Supplementary video 1: 3D reconstruction of a representative microglia from a control brain's larvae (**Figure 1A**). 3D images were generated using Imaris software (Biplane Inc., Version 9.5.0). (Link: https://urlz.fr/iPxZ).

Supplementary video 2: 3D reconstruction of a representative microglia from a *scn1Lab*-KD brain's larvae (**Figure 1B**). 3D images were generated using Imaris software (Biplane Inc., Version 9.5.0). (Link: https://urlz.fr/iPxP).

Supplementary video 3: Time-lapse of 4 dpf control larvae dorsal view showing microglial displacement and processes dynamic (**Figure 2A**). Interval between frames: 39 s. Video played at x6. Microglial tracking displacement was performed using Imaris software (Biplane Inc., Version 9.5.0). (Link: https://urlz.fr/iOIz).

Supplementary video 4: Time-lapse of 4 dpf *scn1Lab* larvae dorsal view showing microglial displacement and processes dynamic (**Figure 2B**). Interval between frames: 39 s. Video played at x6. Microglial tracking displacement was performed using Imaris software (Biplane Inc., Version 9.5.0). (Link: https://urlz.fr/iOIA).

Supplementary Video 5: Representative time-lapse recording of calcium activity in the optic tectum of control larvae (**Figure 4B –** control with microglia). Interval between frames: 200 ms. Video played at x5.

Supplementary Video 6: Representative time-lapse recording of calcium activity in the optic tectum of *scn1Lab*-KD larvae (**Figure 4B –** *scn1Lab*-KD with microglia). Interval between frames: 200 ms. Video played at x5.

Supplementary Video 7: Representative time-lapse recording of calcium activity in the optic tectum of control larvae without microglia (**Figure 4B –** control w/o microglia). Interval between frames: 200 ms. Video played at x5.

Supplementary Video 8: Representative time-lapse recording of calcium activity in the optic tectum of *scn1Lab*-KD larvae without microglia (**Figure 4B –** *scn1Lab*-KD w/o microglia). Interval between frames: 200 ms. Video played at x5.

Supplementary table

il-1β	Forward	5'-CTT AAC CAG CTC TGA AAT GAT G-3'
	Reverse	5'-TGT CGC ATC TGT AGC TCA TTG-3'
il-8	Forward	5'-TGA CCA TCA TTG AAG GAA TGA G-3'
	Reverse	5'-CAT CAA GGT GGC AAT GAT CTC-3'
tnf-α	Forward	5'-TCA CGC TCC ATA AGA CCC AG-3'
	Reverse	5'-GAT GTG CAA AGA CAC CTG GC-3'
il-4	Forward	5'-GAG ACA GGA CAC TAC TCT AAG-3'
	Reverse	5'-GTT TCC AGT CCC GGT ATA TG-3'
il-10	Forward	5'-AAC GAG ATC CTG CAT TTC TAC-3'
	Reverse	5'-CCT CTT GCA TTT CAC CAT AT-3'
tgf-β3	Forward	5'-AAA ACG CCA GCA ACC TGT TC-3'
	Reverse	5'-CCT CAA CGT CCA TCC CTC TG-3'

Graphical Abstract

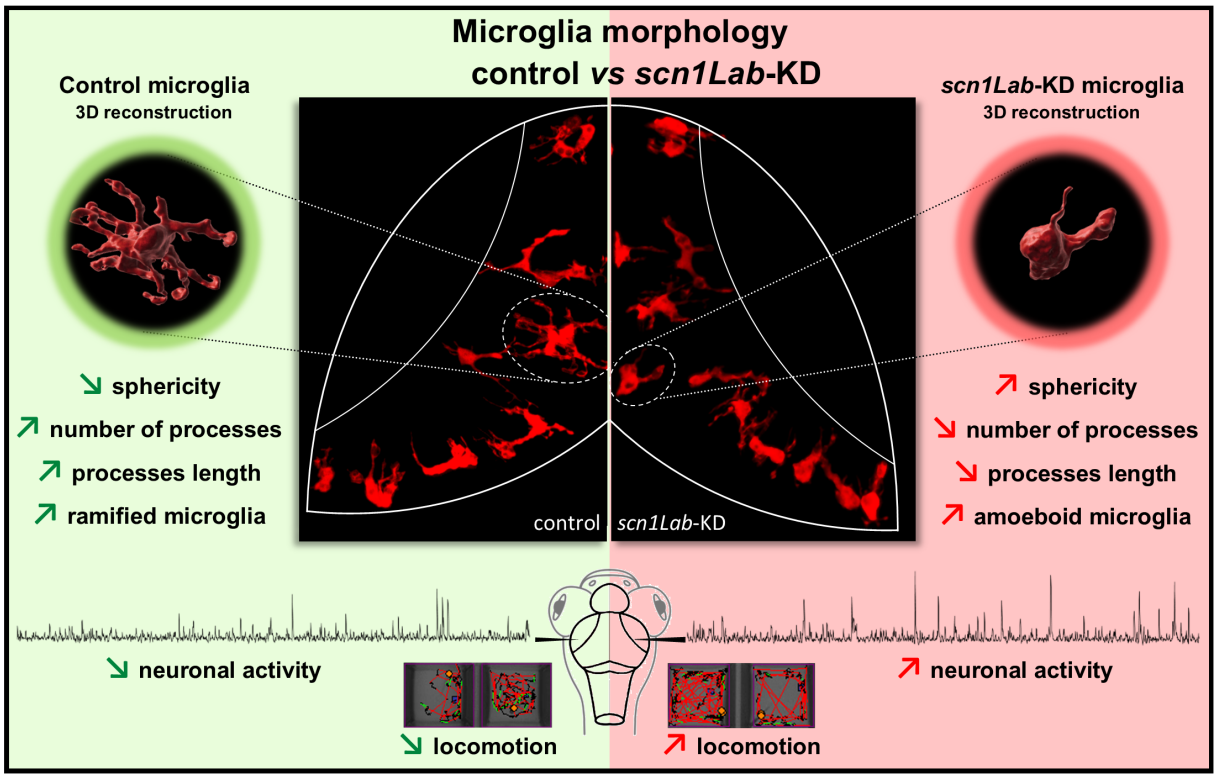

References

Akerboom, J. *et al.* (2012) 'Optimization of a GCaMP calcium indicator for neural activity imaging', *Journal of Neuroscience*. Society for Neuroscience, 32(40), pp. 13819–13840. doi: 10.1523/JNEUROSCI.2601-12.2012.

Altmann, A. *et al.* (2022) 'A systems-level analysis highlights microglial activation as a modifying factor in common epilepsies', *Neuropathology and Applied Neurobiology*, 48(1). doi: 10.1111/nan.12758.

Andoh, M., Ikegaya, Y. and Koyama, R. (2019) 'Synaptic Pruning by Microglia in Epilepsy', *Journal of Clinical Medicine*. MDPI AG, 8(12), p. 2170. doi: 10.3390/jcm8122170.

Avignone, E. *et al.* (2015) 'Altered morphological dynamics of activated microglia after induction of status epilepticus.', *Journal of neuroinflammation*. Journal of Neuroinflammation, 12(1), p. 202. doi: 10.1186/s12974-015-0421-6.

Badimon, A. *et al.* (2020) 'Negative feedback control of neuronal activity by microglia', *Nature*. Nature Research, 586(7829), pp. 417–423. doi: 10.1038/s41586-020-2777-8.

Baraban, Scott C, Dinday, M. T. and Hortopan, G. A. (2013) 'Drug screening in Scn1a zebrafish mutant identifies clemizole as a potential Dravet syndrome treatment.', *Nature communications*, 4, p. 2410. doi: 10.1038/ncomms3410.

Baraban, Scott C., Dinday, M. T. and Hortopan, G. A. (2013) 'Drug screening in Scn1a zebrafish mutant identifies clemizole as a potential Dravet syndrome treatment', *Nature Communications*. Nature Publishing Group, 4(1), p. 2410. doi: 10.1038/ncomms3410.

Benson, M. J., Manzanero, S. and Borges, K. (2015) 'Complex alterations in microglial M1/M2 markers during the development of epilepsy in two mouse models', *Epilepsia*. Blackwell Publishing Inc., 56(6), pp. 895–905. doi: 10.1111/epi.12960.

Boer, K. *et al.* (2008) 'Inflammatory processes in cortical tubers and subependymal giant cell tumors of tuberous sclerosis complex', *Epilepsy Research*. Elsevier, 78(1), pp. 7–21. doi: 10.1016/j.eplepsyres.2007.10.002.

Brenet, A. *et al.* (2019) 'Defective Excitatory/Inhibitory Synaptic Balance and Increased Neuron Apoptosis in a Zebrafish Model of Dravet Syndrome', *Cells*. MDPI AG, 8(10), p. 1199. doi: 10.3390/cells8101199.

Brunklaus, A., Dorris, L. and Zuberi, S. M. (2011) 'Comorbidities and predictors of health-related quality of life in Dravet syndrome', *Epilepsia*. Epilepsia, 52(8), pp. 1476–1482. Available at: https://pubmed.ncbi.nlm.nih.gov/21668444/ (Accessed: 24 April 2021).

Claes, L. *et al.* (2001) 'De Novo Mutations in the Sodium-Channel Gene SCN1A Cause Severe Myoclonic Epilepsy of Infancy', *Am. J. Hum. Genet*, 68, pp. 1327–1332. doi: 10.1086/320609.

Dravet, C. (2011) 'Dravet syndrome history', *Developmental Medicine and Child Neurology*. Dev Med Child Neurol, pp. 1–6. doi: 10.1111/j.1469-8749.2011.03964.x.

Ellett, F. *et al.* (2011) 'mpeg1 promoter transgenes direct macrophage-lineage expression in zebrafish', *Blood*. The American Society of Hematology, 117(4), p. e49. doi: 10.1182/blood-2010-10-314120.

Eyo, U. B. *et al.* (2014) 'Neuronal Hyperactivity Recruits Microglial Processes via Neuronal NMDA Receptors and Microglial P2Y12 Receptors after Status Epilepticus', *Journal of Neuroscience*, 34(32), pp. 10528–10540. doi: 10.1523/JNEUROSCI.0416-14.2014.

Fisher, R. S. *et al.* (2014) 'ILAE Official Report: A practical clinical definition of epilepsy', *Epilepsia*. Blackwell Publishing Inc., 55(4), pp. 475–482. doi: 10.1111/epi.12550.

Fisher, R. S. (2015) 'Redefining epilepsy', *Current Opinion in Neurology*, 28(2), pp. 130–135. doi: 10.1097/WCO.0000000000000174.

Gasmi, N. *et al.* (2021) 'Low grade inflammation in the epileptic hippocampus contrasts with explosive inflammation occurring in the acute phase following status epilepticus in rats: translation to patients with epilepsy', *bioRxiv*. Cold Spring Harbor Laboratory, p. 2021.03.25.436701. doi: 10.1101/2021.03.25.436701.

Hassan-Abdi, R. *et al.* (2019) 'Neurons Expressing Pathological Tau Protein Trigger Dramatic Changes in Microglial Morphology and Dynamics', *Frontiers in Neuroscience*. Frontiers Media S.A., 13. doi: 10.3389/fnins.2019.01199.

He, Y. *et al.* (2018) 'RNA sequencing analysis reveals quiescent microglia isolation methods from postnatal mouse brains and limitations of BV2 cells', *Journal of Neuroinflammation*, 15(1). doi: 10.1186/s12974-018-1195-4.
Kwan, P., Schachter, S. C. and Brodie, M. J. (2011) 'Drug-Resistant Epilepsy', *New England Journal of Medicine*, 365(23), pp. 2238–2240. doi: 10.1056/NEJMC1111683.
Leal, B. *et al.* (2017) 'Brain expression of inflammatory mediators in Mesial Temporal Lobe Epilepsy patients', *Journal of Neuroimmunology*, 313, pp. 82–88. doi: 10.1016/j.jneuroim.2017.10.014.
Li, Y., Du, X., *et al.* (2012) 'Reciprocal Regulation between Resting Microglial Dynamics and Neuronal Activity In Vivo', *Developmental Cell*, 23(6), pp. 1189–1202. doi: 10.1016/j.devcel.2012.10.027.
Li, Y., Du, X. F., *et al.* (2012) 'Reciprocal Regulation between Resting Microglial Dynamics and Neuronal Activity In Vivo', *Developmental Cell*. Cell Press, 23(6), pp. 1189–1202. doi: 10.1016/j.devcel.2012.10.027.
Liu, J. and Baraban, S. C. (2019) 'Network properties revealed during multi-scale calcium imaging of seizure activity in Zebrafish', *eNeuro*. Society for Neuroscience, 6(1). doi: 10.1523/ENEURO.0041-19.2019.
Lukens, J. R. and Eyo, U. B. (2022) 'Microglia and Neurodevelopmental Disorders', *Annual Review of Neuroscience*, 45(1). doi: 10.1146/annurev-neuro-110920-023056.
Marxer, C. A. *et al.* (2021) 'A review of the evidence on the risk of congenital malformations and neurodevelopmental disorders in association with antiseizure medications during pregnancy', *Expert Opinion on Drug Safety*, 20(12), pp. 1487–1499. doi: 10.1080/14740338.2021.1943355.
Maupu, C. *et al.* (2021) 'Diisopropylfluorophosphate-induced status epilepticus drives complex glial cell phenotypes in adult male mice', *Neurobiology of Disease*, 152. doi: 10.1016/j.nbd.2021.105276.
Mildner, A. (2017) 'Ghosts in the shell: Identification of microglia in the human central nervous system by p2y12 receptor', *Neural Regeneration Research*, pp. 570–571. doi: 10.4103/1673-5374.205090.
Mirrione, M. M. *et al.* (2010) 'Microglial ablation and lipopolysaccharide preconditioning affects pilocarpine-induced seizures in mice', *Neurobiology of Disease*. Neurobiol Dis, 39(1), pp. 85–97. doi: 10.1016/j.nbd.2010.04.001.
Morin-Brureau, M. *et al.* (2018) 'Microglial phenotypes in the human epileptic temporal lobe', *Brain*, 141, pp. 3343–3360. doi: 10.1016/0038-1098(79)91043-3.
Nakajima, K. and Kohsaka, S. (2001) 'Microglia: Activation and their significance in the central nervous system', *Journal of Biochemistry*. Oxford University Press, pp. 169–175. doi: 10.1093/oxfordjournals.jbchem.a002969.
Nguyen-Chi, M. *et al.* (2015) 'Identification of polarized macrophage subsets in zebrafish', *eLife*. eLife Sciences Publications Ltd, 4(JULY 2015). doi: 10.7554/eLife.07288.
Di Nunzio, M. *et al.* (2021) 'Microglia proliferation plays distinct roles in acquired epilepsy depending on disease stages', *Epilepsia*, 62(8), pp. 1931–1945. doi: 10.1111/epi.16956.
Peri, F. and Nüsslein-Volhard, C. (2008) 'Live Imaging of Neuronal Degradation by Microglia Reveals a Role for v0-ATPase a1 in Phagosomal Fusion In Vivo', *Cell*. Elsevier B.V., 133(5), pp. 916–927. doi: 10.1016/j.cell.2008.04.037.
Rana, A. and Musto, A. E. (2018) 'The role of inflammation in the development of epilepsy', *Journal of Neuroinflammation*. BioMed Central Ltd. doi: 10.1186/s12974-018-1192-7.
Ravizza, T. *et al.* (2008) 'Innate and adaptive immunity during epileptogenesis and spontaneous seizures: Evidence from experimental models and human temporal lobe epilepsy', *Neurobiology of Disease*. Academic Press, 29(1), pp. 142–160. doi: 10.1016/j.nbd.2007.08.012.
Rhodes, J. *et al.* (2005) 'Interplay of pu.1 and Gata1 determines myelo-erythroid progenitor cell fate in zebrafish', *Developmental Cell*, 8(1), pp. 97–108. doi: 10.1016/j.devcel.2004.11.014.
Salgueiro-Pereira, A. R. *et al.* (2019) 'A two-hit story: Seizures and genetic mutation interaction sets phenotype severity in SCN1A epilepsies', *Neurobiology of Disease*.

Academic Press Inc., 125, pp. 31–44. doi: 10.1016/j.nbd.2019.01.006.
Satta, V. *et al.* (2021) 'Neuropathological Characterization of a Dravet Syndrome Knock-In Mouse Model Useful for Investigating Cannabinoid Treatments', *Frontiers in Molecular Neuroscience*. Frontiers Media S.A., 13, p. 602801. doi: 10.3389/fnmol.2020.602801.
Schoonheim, P. J. *et al.* (2010) 'Optogenetic localization and genetic perturbation of saccade-generating neurons in Zebrafish', *Journal of Neuroscience*, 30(20), pp. 7111–7120. doi: 10.1523/JNEUROSCI.5193-09.2010.
Sieger, D. *et al.* (2012) 'Long-Range Ca2+ Waves Transmit Brain-Damage Signals to Microglia', *Developmental Cell*. Dev Cell, 22(6), pp. 1138–1148. doi: 10.1016/j.devcel.2012.04.012.
Somkhit, J., Yanicostas, C. and Soussi-Yanicostas, N. (2022) 'Microglia Remodelling and Neuroinflammation Parallel Neuronal Hyperactivation Following Acute Organophosphate Poisoning', *International Journal of Molecular Sciences*, 23(15). doi: 10.3390/ijms23158240.
Stafstrom, C. E. and Carmant, L. (2015) 'Seizures and epilepsy: An overview for neuroscientists', *Cold Spring Harbor Perspectives in Biology*, 7(5), pp. 1–19. doi: 10.1101/cshperspect.a022426.
Thurman, D. J. *et al.* (2011) 'Standards for epidemiologic studies and surveillance of epilepsy', *Epilepsia*, 52(SUPPL. 7), pp. 2–26. doi: 10.1111/j.1528-1167.2011.03121.x.
Travnickova, J. *et al.* (2015) 'Primitive macrophages control HSPC mobilization and definitive haematopoiesis', *Nature Communications*, 6, pp. 1–9. doi: 10.1038/ncomms7227.
Vezzani, A. *et al.* (1999) 'Interleukin-1β immunoreactivity and microglia are enhanced in the rat hippocampus by focal kainate application: Functional evidence for enhancement of electrographic seizures', *Journal of Neuroscience*, 19(12), pp. 5054–5065. doi: 10.1523/jneurosci.19-12-05054.1999.
Vezzani, A. *et al.* (2004) 'Functional role of proinflammatory and anti-inflammatory cytokines in seizures', *Advances in Experimental Medicine and Biology*, 548, pp. 123–133. doi: 10.1007/978-1-4757-6376-8_10.
Vezzani, A. *et al.* (2008) 'Glia as a source of cytokines: Implications for neuronal excitability and survival', *Epilepsia*. John Wiley & Sons, Ltd, 49(SUPPL. 2), pp. 24–32. doi: 10.1111/j.1528-1167.2008.01490.x.
Vezzani, A. (2013) 'Fetal brain inflammation may prime hyperexcitability and behavioral dysfunction later in life', *Annals of Neurology*, 74(1), pp. 1–3. doi: 10.1002/ana.23930.
Vezzani, A., Balosso, S. and Ravizza, T. (2019) 'Neuroinflammatory pathways as treatment targets and biomarkers in epilepsy', *Nature Reviews Neurology*. Nature Publishing Group, pp. 459–472. doi: 10.1038/s41582-019-0217-x.
Vinet, J. *et al.* (2012) 'Neuroprotective function for ramified microglia in hippocampal excitotoxicity', *Journal of Neuroinflammation*. BioMed Central, 9. doi: 10.1186/1742-2094-9-27.
Woodburn, S. C., Bollinger, J. L. and Wohleb, E. S. (2021) 'The semantics of microglia activation: neuroinflammation, homeostasis, and stress', *Journal of Neuroinflammation*, 18(1), p. 258. doi: 10.1186/s12974-021-02309-6.
World Health Organization (2019) *Epilepsy*.
Wu, Y. W. *et al.* (2015) 'Incidence of dravet syndrome in a US population', *Pediatrics*. American Academy of Pediatrics, 136(5), pp. e1310–e1315. doi: 10.1542/peds.2015-1807.
Xue-Ping, W. *et al.* (2019) 'Risk factors for drug-resistant epilepsy: A systematic review and meta-analysis', *Medicine (United States)*, 98(30), p. e16402. doi: 10.1097/MD.0000000000016402.
Zhang, Y. *et al.* (2015) 'Pharmacological Characterization of an Antisense Knockdown Zebrafish Model of Dravet Syndrome: Inhibition of Epileptic Seizures by the Serotonin Agonist Fenfluramine', *PLOS ONE*. Edited by Y. Herault. Public Library of Science, 10(5), p. e0125898. doi: 10.1371/journal.pone.0125898.